Arch. Metall. Mater. **66** (2021), 2, 391-396

DOI: 10.24425/amm.2021.135870

U. ELAIYARASAN[1*], V. SATHEESHKUMAR[2], C. SENTHILKUMAR[3]

A STUDY ON TRIBOLOGICAL BEHAVIOUR OF ELECTRO DISCHARGE DEPOSITED ZE41A MAGNESIUM ALLOY USING WEAR MAP

The paper studied the tribological behaviour of electro discharge deposited ZE41A magnesium alloy using wear map. The wear experiments are conducted using pin on disc technique for different parameters such as applied load (1.5 kg-3.5 kg), sliding speed (100 rpm-200 rpm) and sliding time (3 min-7 min). Wear mechanism map is constructed by taking the applied load on y-axis and sliding speed on x-axis. The wear mechanism map is utilized to study the dominance of particular wear mechanism that dominates particular wear regimes such as mild wear, severe wear and ultra severe wear. It is observed that the wear rate increased with increased the applied load and sliding speed. Various mechanisms such as abrasion, oxidation, delamination and melting are identified through scanning electron microscope (SEM).

Keywords: ZE41A magnesium alloy, Electro discharge deposition, Wear mechanism map, mild wear, abrasion

1. Introduction

In recent year, magnesium alloy is widely used in the automobile and aircraft field due to light weight and high strength. Magnesium alloy also have the various advantages such as castability, machinability, bio-compatibility, high thermal conductivity, high dimensional stability, and is easily recycled with low energy consumption. When magnesium alloyed with other material, it possesses superior mechanical properties. Magnesium alloys offer promising alternatives to aluminium [1,2]. Despite the attractive range of properties, it is susceptible to wear and corrosion. Due to its poor wear properties, the application of magnesium alloy is limited [3]. Subsequently, when the corrosion and wear resistance of magnesium alloys increased, the usage will become widespread. Surface modification by coatings has become an important action to enhance the surface properties such as wear, corrosion and oxidation [4]. Algodi et al. [5] have studied the tribological behaviour of high speed steel (HSS) and 304 stainless steel surface coated with TiC/Fe powder metallurgy semi sintered electrode by electrical discharge coating. The wear test was performed by in-house linear reciprocating ball-on-flat tribometer and with wear parameters viz., normal applied loads (10 N and 50 N) and wear track length (10 mm) on the response wear rate and coefficient of friction. It was found that the wear rate and coefficient of friction increases with increase in normal load for TiC coating on HSS. Selvam et al. [6] have investigated the dry sliding wear behaviour of AA6061 aluminium alloy containing 0, 4, 8 and 12 wt. % of fly ash particles. Wear tests were conducted under different load (4.9, 9.8, 14.7, 19.6, and 24.5 N), sliding velocity (1.57 m s^{-1}), sliding distance (4000 m) and track radius (100 mm). It was found that the wear rate increases with increase in fly ash particle in the composite. Composites exhibit better wear resistance compared to unreinforced alloy up to a load of 24.5 N. Baradeswaran et al. [7] have analysed the optimization of wear behaviour of Al-Al_2O_3 Composites. The wear test was conducted using pin-on-disc technique with the controlled parameters such as applied load of 10, 20, 30, and 40 N, sliding distance of 1200 m and sliding speed of 0.6 m/s. It was concluded that the wear resistance increased with addition of the Al_2O_3 particle content in the composite. Ghosh et al. [8] have optimized the wear characteristics of Al-7.5%SiC metal matrix composite by Taguchi analysis. The samples were tested in a Multi-Tribotester (DUCOM TR-25) using a block on roller arrangement at different testing parameters such applied load, speed and time. The SEM study of the wear tracks revealed that mostly abrasive wear phenomenon is encountered. Şahin [9] have investigated the wear behaviour of SiC/2014 aluminium composite. The wear experiments were conducted with pin on

[1] DEPARTMENT OF MECHANICAL ENGINEERING, KARPAGA VINAYAGA COLLEGE OF ENGINEERING AND TECHNOLOGY, MADHURANTHAGAM, INDIA-603308
[2] DEPARTMENT OF MECHANICAL ENGINEERING, GOVERNMENT COLLEGE OF ENGINEERING, SALEM, INDIA – 636011.
[3] DEPARTMENT OF MECHANICAL ENGINEERING, UNIVERSITY COLLEGE OF ENGINEERING, PANRUTI- 607106, INDIA

* Corresponding author: elaiyarasan555@gmail.com

disc apparatus under different parameters such as abrasive grain size, normal load and sliding distance. Wear rate of the composite increases with increase in load and sliding distance. It was found that the abrasive grain size exerted the greatest effect on the wear, followed the hardness.

From the recent survey, many researches focused on the wear behaviour of different material but few research works were found on the wear behaviour of coated materials. In this present investigation, ZE41A magnesium alloy has been coated with tungsten carbide-copper (WC/Cu) material using electrical discharge coating (EDC). Hence, the wear mechanism of WC/Cu coated magnesium alloy was investigated. Further wear transition and wear mechanism maps are drawn to determine the various wear regimes. Different wear mechanism are found from the worn coated specimen through scanning electron microscope (SEM) and Energy dispersive spectroscopy (EDS) analysis has been carried out to find the elements presents in the coated surface of workpiece.

2. Experimental details

2.1. Materials, methods and Equipments

In this investigation, ZE41A magnesium alloy was selected as base material and its chemical composition has been given in Table 1. The tungsten carbide (WC) and copper (Cu) powder particles with particle size of 4 μm were selected as the electrode material because of high strength and high electrical conductivity. The powders were mixed in the combination of 50:50 (wt.%) and compacted using powder metallurgy route under different loads. Consequently, the prepared green compact electrode was sintered about 600°C for 20 min using tubular furnace under argon atmosphere condition. Then the sintered electrodes have been cooled in the furnace. The prepared electrode was polished and buffed to make it flat prior to experimentation. Further, the experiments were conducted with prepared electrode using conventional die sinking EDM machine with EDM oil as dielectric. Finally, the experiments were carried out using constant voltage of 40 V, inter electrode gap of 0.5 mm, compaction load of 150 MPa, current of 3 A and pulse time of 86 μs with fixed time interval of 10 min.

TABLE 1

Chemical composition of ZE41A Magnesium alloy (wt.%)

Si	Cu	Zn	Zr	Fe	TRE	Ni	Mn	Al	Mg
0.003	0.002	3.80	0.60	0.004	1.18	0.002	0.003	0.006	Bal

2.2. Preparation of pin and disc

The WC/Cu coated ZE41A magnesium alloy was machined with diameter of 10 mm and length of 20 mm. The counterface disc was made of EN31 steel material with 50 mm diameter. The hardness of the disc was 65HRC and it was smoothened well with abrasive emery sheet of 1000 grade. The prepared wear pin samples and counterface disc is shown in Fig. 1(a) and (b). The flatness and perpendicular orientation of the pin surfaces were checked to ensure that the pins at perfectly on the disc surface.

2.3. Wear test

All experiments were conducted in air at (28 ± 1)°C according to ASTM: G99 in a DUCOM pin on disc wear testing machine (TR-20-PHM-M1) is shown in Fig. 2. The wear pin samples were set in a slot in the arm above the counterface disc. The surface contact between the pin and disc surface was maintained at 100%. The experiments were conducted under applied loads (1.5 kg, 2.5 kg and 3.5 kg), sliding speed (100 rpm, 200 rpm and 300 rpm), sliding time (3 min, 5 min and 7 min) and the rack diameter of 20 mm. At the end of every sliding interval, the pins have been carefully cleaned using acetone to remove the burrs and particles produced during the sliding of the pin on the disc surfaces. The exact mass of the pin was measured after the wear debris on the pin surface was removed, and the mass losses were calculated at every sliding interval. The specific wear rate of experiments was calculated by the given formula

$$Ws = \Delta m/\rho \,.\, t \,.\, F_N \,.\, Vs \ (\mathrm{mm^3/N–m}) \qquad (1)$$

Where Δm is the mass losses of the pin samples (g), ρ is the density of the test sample (g/mm^3), t is the sliding time (s), Vs is the sliding speed (m/s), F_N is the Applied load (N).

Fig. 1. (a) Wear pin samples, and (b) counterpart disc made of EN31 steel

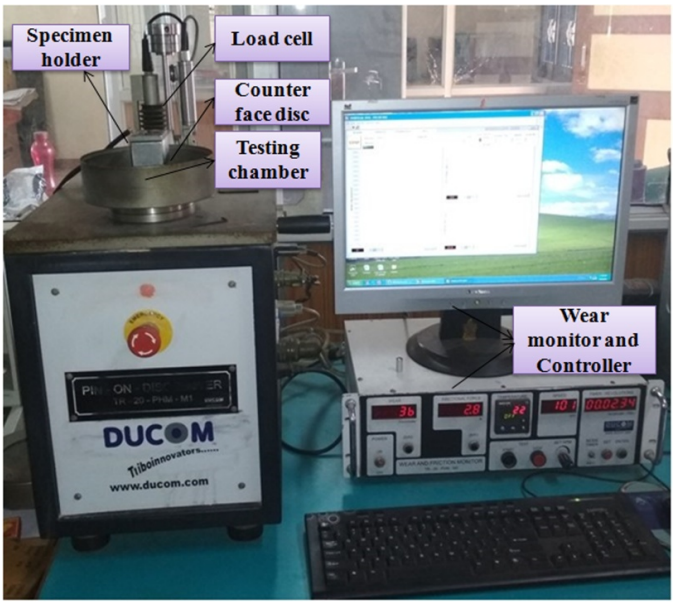

Fig. 2. Pin on disc apparatus

Prior to each test, the disc was ground with 1000-grit SiC paper and then cleaned using acetone to remove the accumulated particles on the disc surface due to the prior sliding of the pin surface. The experiments were repeated thrice to minimize the possible experimental error and error bars. All worn pin surfaces were analysed using scanning electron microscopy (SEM) to identify the different wear mechanism.

2.4. Experimental design and ANOVA

The experiment was carried out to analyse the effect of Sliding parameters on wear rate of ZE41A magnesium alloy coated with WC/Cu composite. In the present investigation, standard Taguchi L9 (3^3) orthogonal array was chosen. The process parameters and their levels are given in Table 2. The wear experiments were conducted as per the design developed by taguchi method and values of wear rate was recorded in the Table 3. ANOVA test was conducted at a confidence level of 95 % and significance level of 5%, to determine the significant level of each input process parameter, which influenced the wear characteristics as shown in Table.4. From the results of ANOVA, it was disclosed that the sliding speed was the most significant factor. The applied load was the least influential parameters on the wear characteristics.

TABLE 2

Control factors and their levels

Control factors	Unit	Level		
		I	II	III
Applied load	kg	1.5	2.5	3.5
Sliding speed	rpm	100	200	300
Sliding time	min	3	5	7

TABLE 3

Wear rate results for WC/Cu coated magnesium alloy

Ex. No	Control factors			Wear rate (mm^3/N-m)
	Applied load (kg)	Sliding speed (rpm)	Sliding time (min)	
1	1.5	100	3	0.0002490
2	1.5	200	5	0.0002947
3	1.5	300	7	0.0003810
4	2.5	100	5	0.0002849
5	2.5	200	7	0.0003610
6	2.5	300	3	0.0003415
7	3.5	100	7	0.0003959
8	3.5	200	3	0.0002792
9	3.5	300	5	0.0004358

TABLE 4

Analysis of Variance of wear rate

Source	DF	Adj SS	Adj MS	F-Value	Percentage Contribution (%)
Applied load (kg)	2	0.000060	0.000030	3.01	20.39
Sliding speed (rpm)	2	0.000113	0.000057	5.71	38.68
Sliding time (min)	2	0.000120	0.000060	6.04	40.92
Error	2	0.000020	0.000010		
Total	8	0.000313			

3. Result and discussion

3.1. Microstructure of the WC/Cu coating

SEM micrographs were taken from the top surface of the coated surface as shown in Fig. 3(a). The coated surface showed that the EDC process formed the microvoids and craters on the surface. It was cleared from the SEM photographs that with the increment of compaction load, the surface morphology of the coating becomes more uneven/non-uniform and the material coating takes place in the form of globules. Fig. 3(b) shows the EDS peak plot of the corresponding coated surface. It was cleared from the EDS plot that the electrode material equally deposited on the workpiece with weight percentage of 0.16 W and 0.16 Cu. Layer thickness of the coated surface was taken from the cross section of the coating as shown in Fig. 3(c). Average coating thickness of 85.60 µm was achieved at compaction load 150 MPa, current 3A and pulse on time 86 µs.

3.2. Wear rate map

Wear rate map is necessary to identify the wear properties of desired material under various sliding conditions. Wear rate map is used to study the influence of sliding parameters such as Applied load and sliding speed on wear rate. The wear rate map has been constructed using Minitab software by considering ap-

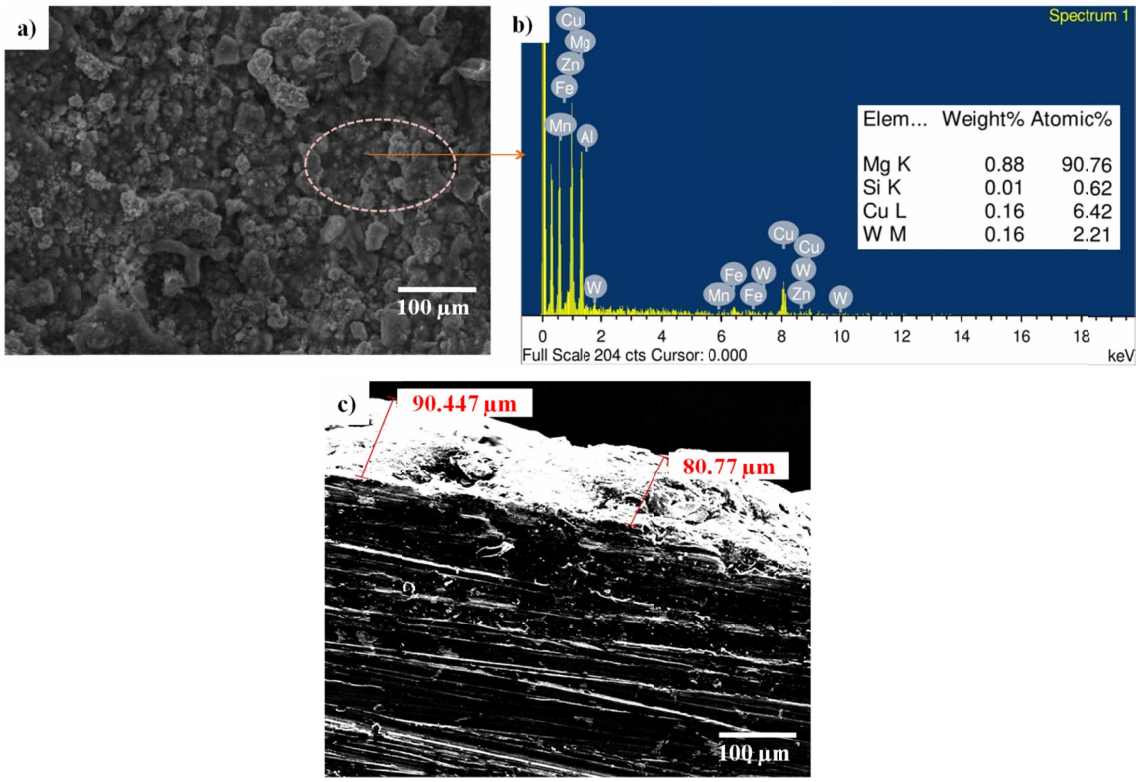

Fig. 3. (a) SEM microstructure of WC/Cu coating at 150MPa, 3A and 86 µs, and (b) EDS plot for WC/Cu coating. (c) Layer thickness of WC/Cu coating

plied load on Y-axis and sliding speed on X-axis, which resulted in the wear rate on *Z*-axis. The adjustment in the direction of contour lines represents the mode of wear such as mild wear, severe wear and ultra severe wear. Every contour line represents the wear rate for different applied load and sliding speed. Wear rate map of WC/Cu coated ZE41A magnesium alloy as shown in Fig. 4. From wear rate map, it is showed that the vertical contour line indicates the effect of applied load and horizontal contours indicates the effect of sliding speed. In this plot, wear rates increases with increase in the applied load and sliding speed. At high sliding speeds, large variations in the slopes of the wear rate curves. The slope changed coincided with the transition from mild wear to severe wear. Hence, the wear rate of the coated magnesium alloy is minimum in the lower applied load and sliding speed and maximum at higher applied load and sliding speed.

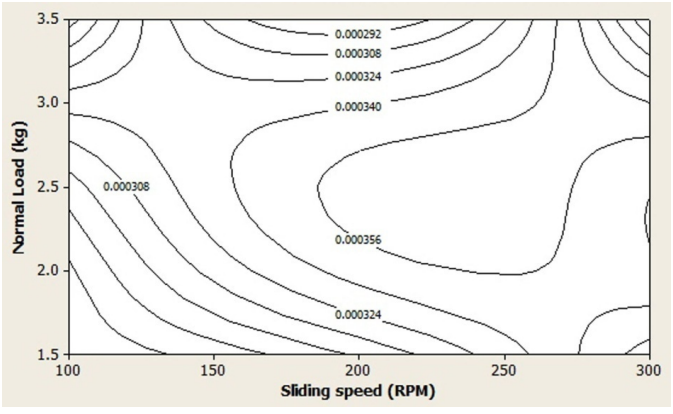

Fig. 4. Wear rate map for WC/Cu coated magnesium alloy

3.3. Wear transition map

Wear transition map offers the context to study about different wear mechanisms in each region for various dry sliding parameters. Boundary surface of predominant wear and their transitions is essential for constructing the wear transition map. The wear transition map explains the minimum number of wear mechanisms in the given working conditions. By investigating the wear contour maps, it was observed that the equal line spacing and lack of curvature typically indicate the same dominant mechanism. Valley and plateaus indicated the changes in the wear mode. In these conditions, different wear mechanisms can be identified in the worn surface regions. Fig. 5 shows the wear transition map for ZE41A magnesium alloy. It illustrates the three different wear regimes such as mild wear, severe wear and ultra severe wear. The transitions of boundary surfaces were formed between mild wear to severe wear and severe to ultra severe wear.

3.4. Wear mechanism map

Wear mechanism map indicates the locations of the dominance of different wear mechanisms and is shown in Fig. 6. The physical wear mechanism maps need extensive physical modelling for determination of boundaries for different mechanisms. In empirical maps, the boundaries are constructed roughly based on the observations of the worn out surface. Because of the wide range of sliding speed and applied load covered by the map, it

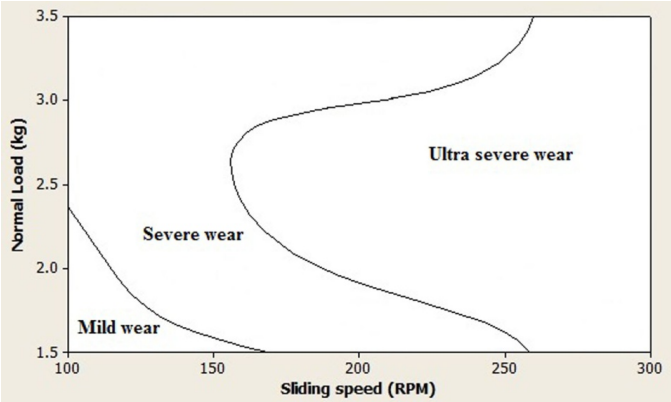

Fig. 5. Wear transition map for WC/Cu coated magnesium alloy

should enable the designer to decide intelligently whether the material under study will be able to meet the set of requirements for a particular tribological application.

The Abrasive wear is formed at workpiece tested in the parameter of applied load of 1.5 kg and sliding speed of 100 rpm and is shown in Fig. 7. This wear is formed due to scratch of hard particles. It usually formed in the systems involving hard particles in relative motion to the contact surface. The abrasive wear depends on the hardness of the abrasive particles. The worn out surface taken from the mild wear region shows mostly grooves, indicative of micro abrasion being the dominant wear mechanism [10]. Oxidation mechnism in depostited surface was identified in pin tested at 1.5 kg and 200 rpm and is shown in Fig. 8. It is characterized by the formation of spots that cover almost the whole surface of the WC/Cu coated magnesium alloy and in some case, a thin oxide layer was formed. The wear debris revealed that the detached hard particles were oxidized vigorously. During sliding, the frictional heating causes oxidation of the surface, therefore the oxidative wear formed due to the removal of the oxide fragments [11]. The presence of this oxidation layer formed during the wear test hinders the contact between the pin and the counterface body and therefore the wear rates were lower in this conditions.

The delamination mechanism is foremed at intermediate applied load of 2.5 kg and sliding speed of 200 rpm. When the predominant wear mechanism is delamination, detachment of the worn surface material is produced in sheet form because the formation of cracks during the wear test that are perpendicular

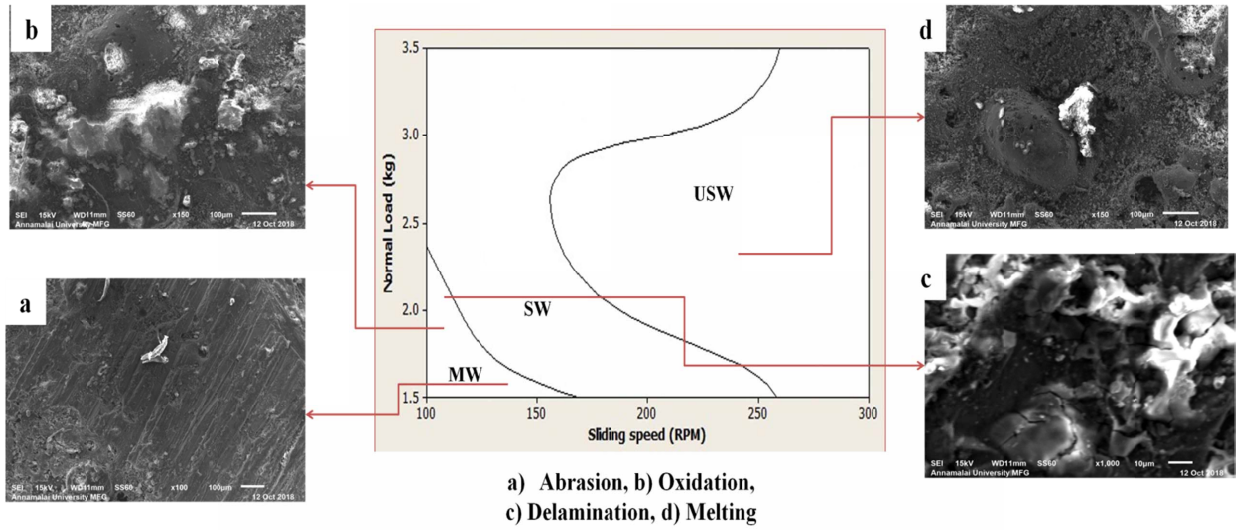

Fig. 6. Wear mechanism map of WC/Cu coated ZE41A magnesium alloy against sliding speed and normal load

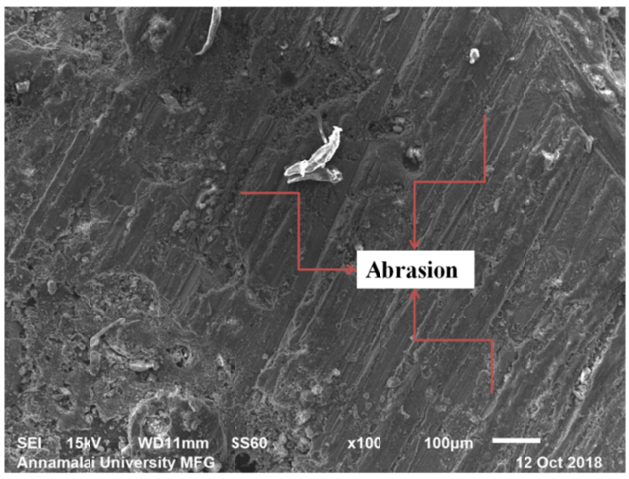

Fig. 7. Abrasion at 1.5 kg and 100 rpm

to the sliding direction and the growth of subsurface cracks that cause the final detachment. Fig. 9 shows the surface morphology of delamination mechanism which indicates the cracks and voids. The examination of the debris of the samples reveals numerous flakes or sheets. Fatigue produced during sliding induces the subsurface deformation, the crack nucleation and the crack propagation [12]. Therefore, the increasing of the applied load accelerates this process and hence delamination wear occurs.

Melting mechanism is formed at the highest applied load of 3.5 kg and sliding speed of 300 rpm. Fig. 10 shows the surface morphology of the melting mechanism, in which the highest applied load and sliding speed increased the local temperature between the pin and the counterbody [13], which resulted the melting of the deposited magnesium alloy. Hence the improvement of wear resistrance does not occur at these conditions.

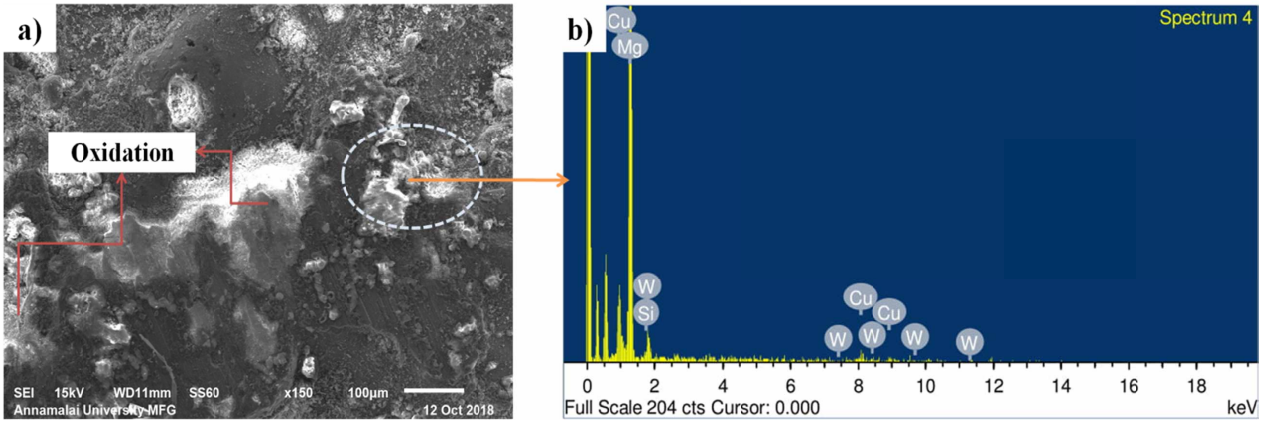

Fig. 8. Oxidation at 1.5 kg and 200 rpm

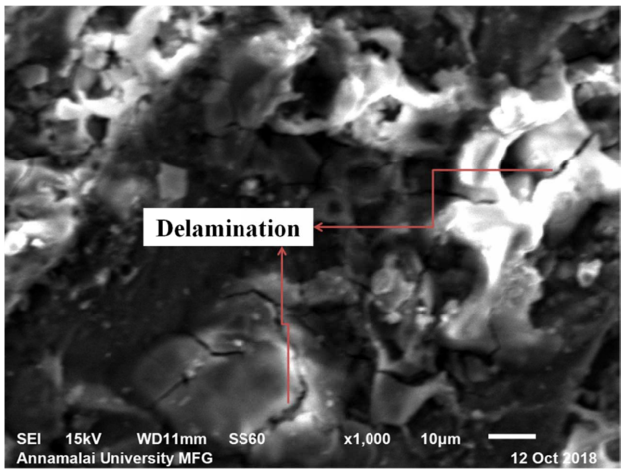

Fig. 9. Delamination at 2.5 kg and 200 rpm

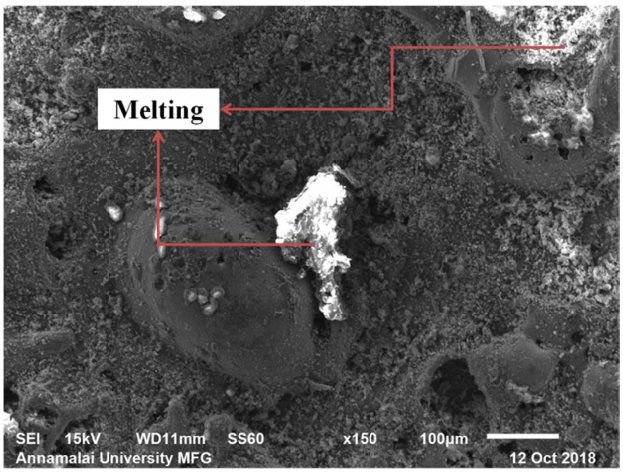

Fig. 10. Melting at 3.5 kg and 300 rpm

4. Conclusion

The tribological behaviour of electro discharge deposited ZE41A magnesium alloy with WC/Cu composite electrode has been studied under different sliding. It was concluded that the wear rate increased with increased the applied load and sliding speed. Wear mechanism map was constructed to indentify the different wear regime such as mild wear, severe wear and ultra severe wear. Different wear mechanisms such as abrasion, oxidation, delamination and melting were indentified using SEM. Most dominant mechanisms is abrasion (1.5 kg and 100 rpm), which was occurred at all experimental condition. Melting mechanism was mostly affected the deposited surface, which was formed at high applied load (3.5 kg) and sliding speed (300 rpm).

REFERENCES

[1] D.K. Him, K.S. Shin, N.J. Kim, Adv. Perform. Mater. **5**, 319-29 (1998).

[2] U. Elaiyarasan, V. Satheeshkumar, C. Senthilkumar, Mater. Res. Exp. **6** (12), 126533 (2019).

[3] J.D. Majumdar, B.R. Chandra, B.L. Mordike, R. Galun, I. Manna, Surf. Coat. Techno. **174**, 1018-1023 (2003).

[4] U. Elaiyarasan, V. Satheeshkumar, C. Senthilkumar, Mater. Res. Exp. **5** (8), 086501 (2018).

[5] S.J. Algodi, J.W. Murray, P.D. Brown, A.T. Clare, Wear. **402**, 109-123 (2018).

[6] J. David Raja Selvam, D.S. Robinson Smart, Kovo. Mater. **54**, 175-183 (2016).

[7] A. Baradeswaran, A. Elayaperumal, R.F. Issac, Proc. Eng. **64**, 973-982 (2013).

[8] S. Ghosh, P. Sahoo, G. Sutradhar, Adv. Mater. Manu. Character. **4** (2), 93-99 (2014).

[9] Y Sahin, Tribo. Int. **43** (5-6), 939-943 (2010).

[10] R.D.M. Castro, A.D.S. Rocha, E.I. Mercado Curi, F. Peruch, Amer. J. Mater. Sci. **8** (1), 15-26 (2018).

[11] D. Rai, B. Singh, J. Singh, Wear. **263** (1-6), 821-829 (2007).

[12] P. Samyn, G. Schoukens, F. Verpoort, J. Van Craenenbroeck, P. De Baets, Macro. Mater. Eng. **292** (5), 523-556 (2007).

[13] U. Elaiyarasan, V. Satheeshkumar, C. Senthilkumar, J. Bio. Tribo. Corr. **5** (1), 30 (2019).